

Band-limited Features in the Primordial Power Spectrum Do Not Resolve the Hubble Tension

MIAOXIN LIU¹ AND ZHIQI HUANG¹

¹*School of Physics and Astronomy, Sun Yat-Sen University, 2 Daxue Road, Tangjia, Zhuhai, 519082, P.R.China*

(Dated: July 17, 2020)

ABSTRACT

For a standard Λ CDM universe with a power-law primordial power spectrum, the discrepancy between early- and late-universe measurements of the Hubble constant continued to grow and recently reached 5.3σ . During inflation, local features in the inflationary potential often lead to band-limited features in the primordial power spectrum, hence breaking the power-law assumption in the derivation of the Hubble tension. We investigate whether such inflationary “glitches” can ease the Hubble tension. The recently released *Planck* temperature and polarization data and the 2019 SH0ES+H0LiCOW joint constraint on the Hubble constant are combined to drive a blind Daubechies wavelet signal search in the primordial power spectrum, up to a resolution $\Delta \ln k \sim 0.1$. We find no significant detection of any features beyond power law. With 64 more degrees of freedom injected in the primordial power spectrum, the Hubble tension persists at a 4.9σ level.

Keywords: cosmology, Hubble constant, CMB, inflation

1. INTRODUCTION

The Λ cold dark matter (Λ CDM) model has been taken as the standard cosmological paradigm since the discovery of late-universe acceleration (Riess et al. 1998; Perlmutter et al. 1999). It is a remarkable success in terms of explaining the temperature and polarization anisotropies of the cosmic microwave background (CMB) that have been accurately measured by the *Planck* satellite (Akrami et al. 2018a; Aghanim et al. 2018), the baryon acoustic oscillation features in the galaxy redshift survey data (Gil-Marín et al. 2016; Abbott et al. 2019), the weak gravitational lensing of galaxies (Troxel et al. 2018), the Type Ia supernovae luminosity distances (Scolnic et al. 2018; Macaulay et al. 2019), and many others.

Recently, the local distance-ladder measurement of Hubble constant (SH0ES) (Riess et al. 2016, 2018a,b; Riess et al. 2019), followed by independent support from time delay of strong-lensing quasars images (H0LiCOW, STRIDES) (Wong et al. 2019; Shajib et al. 2019), starts to challenge the “concordance” Λ CDM picture. Assuming a minimal six-parameter Λ CDM model, SH0ES

and H0LiCOW results together provide a 5.3σ difference of H_0 with the CMB measurement. This inconsistency, often referred to as “Hubble tension”, may indicate new physics beyond Λ CDM. Simple one-parameter extensions of Λ CDM, however, were found insufficient to resolve the Hubble tension (Guo et al. 2019; Miao & Huang 2018). More sophisticated models are hence proposed to take the challenge. The list includes but is not limited to modified gravity (Lin et al. 2019b,a; Sola et al. 2019; Rossi et al. 2019), dark energy with phantom equation of state (Li & Shafieloo 2019; Pan et al. 2019; Panpanich et al. 2019), early dark energy models (Karwal & Kamionkowski 2016; Alexander & McDonough 2019; Poulin et al. 2019), backreaction phenomena (Rácz et al. 2017; Kovács et al. 2020), interacting dark components (Di Valentino et al. 2017; Yang et al. 2018b,a; Di Valentino et al. 2018; Bhattacharyya et al. 2019; Di Valentino et al. 2019), decaying dark matter (Vattis et al. 2019; Blinov et al. 2020), modified recombination history (Chiang & Slosar 2018; Ye & Piao 2020; Liu et al. 2019), primordial magnetic fields (Jedamzik & Pogossian 2020), and extra relativistic species (D’Eramo et al. 2018; Benetti et al. 2017; Benetti et al. 2018; Graef et al. 2019; Carneiro et al. 2019). It has also been claimed that the Hubble tension may just

huangzhq25@mail.sysu.edu.cn

Corresponding author: Zhiqi Huang

be a relativistic non-linear effect in the standard Λ CDM paradigm (Bolejko 2018).

Adhikari and Huterer proposed that non-Gaussian CMB covariance from a strong coupling between long-wavelength modes and short-wavelength modes can resolve the Hubble tension (Adhikari & Huterer 2020). We repeated their calculation and found the same results. However, we noticed that in this model the posterior amplitude of matter fluctuations (σ_8) is significantly higher than Λ CDM value, which is already at the upper edge of the bounds from late-universe observations of galaxy clustering and weak gravitational lensing (Aghanim et al. 2018). Moreover, it is yet to be shown that the prediction of polarization and the large tri-spectrum in this model is consistent with *Planck* data.

Nevertheless, the idea that Hubble tension may be due to some anomalies in primordial conditions is worth further investigation.

In the concordance picture, the initial seeds of cosmological fluctuations are assumed to originate from vacuum quantum fluctuations during early-universe inflation. For simplest single-field slow-roll inflation models, the predicted primordial metric fluctuations are almost perfectly Gaussian, and has a slightly tilted power-law primordial scalar power spectrum $\mathcal{P}(k) = A_s \left(\frac{k}{k_{\text{pivot}}}\right)^{n_s-1}$, where k is the comoving wave number and $k_{\text{pivot}} = 0.05\text{Mpc}^{-1}$ is the pivot scale. The standard analysis of CMB and large-scale structure data is usually established on this featureless power-law primordial power spectrum. The global deviation from power-law shape, is bounded by *Planck* data within a sub-percent level: $\frac{dn_s}{d\ln k} = -0.0041 \pm 0.0067$ (Aghanim et al. 2018), which is fully consistent with the single-field slow-roll prediction $\left|\frac{dn_s}{d\ln k}\right| \lesssim 10^{-3}$. The *Planck* collaboration also studied a broad class of inflation models as well as many phenomenological parametrizations, but found no evidence beyond the single-field slow-roll scenario (Akrami et al. 2018b, 2019). Neither does a blind node expansion with cubic-spline interpolation favor any smooth non-power-law features with a resolution $\Delta \ln k \sim 1$ (Akrami et al. 2018b). These results are supported by many other independent works (Meerburg et al. 2012; Zeng et al. 2019; Domnech & Kamionkowski 2019). In summary, the CMB data do not favor any global periodic oscillations or any broad smooth features with resolution $\Delta \ln k \sim 1$.

The apparently missing ingredient - sharper local features with $\Delta \ln k \ll 1$ are as well motivated from the theoretical perspectives. Note that $\ln k$ roughly corresponds to physical time or number of expansion e-folds

during inflation. Many slow-roll-breaking processes during inflation, such as crossing a step in the inflaton potential, has strong impact only for \sim a few $\times 0.1$ e-folds. These models can then produce sharp ($\Delta \ln k \sim$ a few $\times 0.1$) features that are typically local in time ($\ln k$) domain and band-limited in frequency (Fourier conjugate of $\ln k$) domain. One way to study these sharp features is the top-down approach, that is, to parameterize and constrain the predicted features, in a model-by-model manner. For a few templates from popular models, the *Planck* collaboration, again, found null results (Akrami et al. 2018b). See also Refs. (Hazra et al. 2013; Verde & Peiris 2008; Tocchinivalentini et al. 2006; Handley et al. 2019) for earlier works. The other way, which is missing for the latest Hubble-tension related data, and will be done in this work, is the bottom-up approach that model-independently covers a much broader class of models.

We apply a wavelet analysis, a statistical tool specifically designed to study local and band-limited signals, to search for sharp features in the primordial power spectrum. Similar analysis has been done for earlier CMB data from COBE and WMAP satellites (Pando et al. 1998; Mukherjee et al. 2000; Mukherjee & Wang 2003a,b; Shafieloo et al. 2007), before *Planck* data drove the Hubble tension. The purpose of our re-examination in the latest *Planck* data is to investigate whether the Hubble tension is driven by a primordial sharp feature that manifests itself in high- ℓ multipoles that are only accurately measured by *Planck*.

This paper is organized as follows. In Sec. 2 we introduce Daubechies wavelet analysis and our power spectrum reconstruction method. In Sec. 3 we test the wavelet reconstruction method with mock CMB data for a fiducial inflationary model with slow-roll violation. In Sec. 4 we report the results for *Planck* + SH0ES + H0LiCow data. Sec. 5 concludes.

2. METHOD

The Daubechies wavelet basis takes the form:

$$\Psi_{n,m}(t) = 2^{n/2} \Psi_{0,0}(2^n t - m), \quad n, m \in Z \quad (1)$$

where $\Psi_{0,0}$ is the mother function of Daubechies wavelet. The basis functions are complete, compactly supported and orthogonal with respect to both the scale n and the position m indices. They are moving kernels with hierarchical resolutions, with each resolution level a factor of 2 finer than the previous one. As shown in Fig. 1, the Daubechies mother functions are not unique. The most oft-used 1st order Daubechies mother function, also known as Haar wavelet, is simple but discontinuous. Higher-order Daubechies in general cannot be expressed with elementary functions, but are continuous.

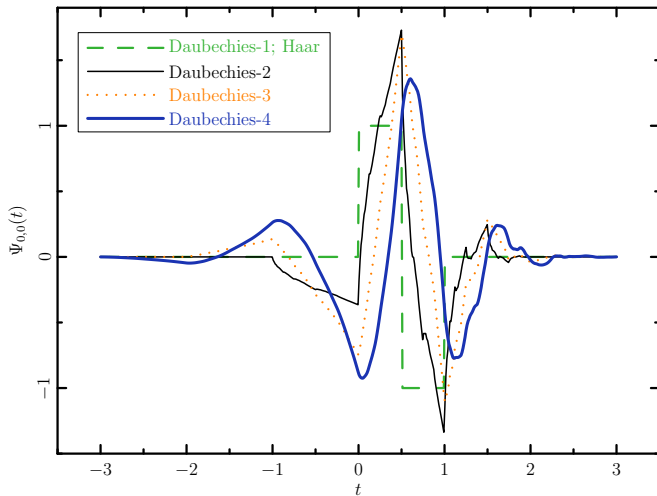


Figure 1. Daubechies wavelet mother functions.

The smoothness of the Daubechies mother function increases with its order. In this work, we use the 4th order Daubechies basis, and check the robustness of our result with second-order Daubechies basis. The algorithm to construct Daubechies mother function of arbitrary order is given in Appendix A.

To blindly search features in the primordial scalar power spectrum $\mathcal{P}(k)$, we decompose its deviation from power-law shape into Daubechies wavelets

$$\ln \frac{\mathcal{P}(k)}{\mathcal{P}_{\text{ref}}(k)} = \sum_{n=0}^3 \sum_{m=-2^{n+1}}^{2^{n+1}-1} A_{n,m} \Psi_{n,m} \left(\ln \frac{k}{k_{\text{pivot}}} \right), \quad (2)$$

where the reference power-law is $\mathcal{P}_{\text{ref}}(k) = A_s \left(\frac{k}{k_{\text{pivot}}} \right)^{n_s-1}$. The lower and upper bounds of the scale index n are chosen such that the resolution in $\ln k$ is limited to $0.1 \lesssim \Delta \ln k \lesssim 1$, to match features from slow-roll-breaking processes during inflation. The lower and upper bounds of the position index m are chosen such that CMB scales measured by *Planck* are well covered.

We use the publicly available software CosmoMC (Lewis & Bridle 2002) to run Markov Chain Monte Carlo (MCMC) simulations and to estimate the marginalized bounds of cosmological parameters, which include the standard six built-in parameters $\Omega_b h^2$, $\Omega_c h^2$, θ , τ_{re} , $\ln(10^{10} A_s)$, n_s and the sixty-four $A_{n,m}$ coefficients defined in Eq. (2). Here $\Omega_b h^2$ and $\Omega_c h^2$ are baryon and CDM densities, respectively; θ is the angular extension of sound horizon on the last scattering surface; τ_{re} is the reionization optical depth; A_s and n_s are the amplitude and index of the primordial scalar power spectrum. The Hubble constant H_0 can be derived from

these parameters. The sum of neutrino masses is fixed to $\sum m_\nu = 0.06 \text{eV}$, the minimum value allowed in normal hierarchy picture. Flat priors are applied to all the parameters including the $A_{n,m}$ coefficients.

The advantage of using wavelets is that they are local by construction. The additional degrees of freedom, despite being many, are not strongly correlated. This significantly accelerates the convergence of MCMC sampling.

3. TEST WITH MOCK DATA

To test the viability of the wavelet reconstruction method, we consider a toy model with inflationary potential

$$V = \frac{3}{4} m^2 M_p^2 \left(1 - e^{-\sqrt{\frac{2}{3}} \frac{\phi}{M_p}} \right)^2 \left(1 + \epsilon e^{-\frac{(\phi-\phi_0)^2}{2\mu^2}} \right), \quad (3)$$

where $M_p = 2.45 \times 10^{18} \text{GeV}$ is the reduced Planck mass. This potential is constructed by adding a small bump, characterized by the amplitude parameter $\epsilon \ll 1$, the position parameter ϕ_0 and the width parameter μ , to the Starobinsky potential (Starobinsky 1983). The parameters $m = 1.191 \times 10^{-5} M_p$, $\phi_0 = 5.37 M_p$, $\mu = 0.005 M_p$, and $\epsilon = 10^{-5}$ are chosen such that, when instant reheating is assumed, the primordial power spectrum roughly matches CMB observations. The small bump leads to a temporary slow-roll violation and a typical width $\Delta \ln k \sim$ a few $\times 0.1$ of the feature in the primordial power spectrum, which we compute by numerically integrating the linear perturbation equations of the gauge-invariant Sasaki-Mukhanov variable (Sasaki 1986; Mukhanov 1988). The other cosmological parameters for the fiducial cosmology are taken to be the *Planck* 2018 best-fit values (Aghanim et al. 2018), as shown in the first column of Table 1.

To generate the mock CMB data, we assume the full width at half maximum (FWHM) = 5 arcmin for the temperature beam resolution, and FWHM = 10 arcmin for polarization. With Gaussian approximation, the mock CMB likelihood reads (Verde et al. 2006)

$$\begin{aligned} \ln \mathcal{L} = & - \frac{f_{\text{sky,eff}}}{2} \sum_{\ell=\ell_{\text{min}}}^{\ell_{\text{max}}} (2\ell+1) \\ & \times \left[\frac{\hat{C}_\ell^{TT} \hat{C}_\ell^{EE} + \hat{C}_\ell^{EE} \hat{C}_\ell^{TT} - 2\hat{C}_\ell^{TE} \hat{C}_\ell^{TE}}{\hat{C}_\ell^{TT} \hat{C}_\ell^{EE} - (\hat{C}_\ell^{TE})^2} \right. \\ & \left. + \ln \left(\frac{\hat{C}_\ell^{TT} \hat{C}_\ell^{EE} - (\hat{C}_\ell^{TE})^2}{\hat{C}_\ell^{TT} \hat{C}_\ell^{EE} - (\hat{C}_\ell^{TE})^2} \right) - 2 \right], \quad (4) \end{aligned}$$

where we have used $\ell_{\text{min}} = 2$, $\ell_{\text{max}} = 2500$, and an effective sky coverage $f_{\text{sky,eff}} = 0.85$. In this formula,

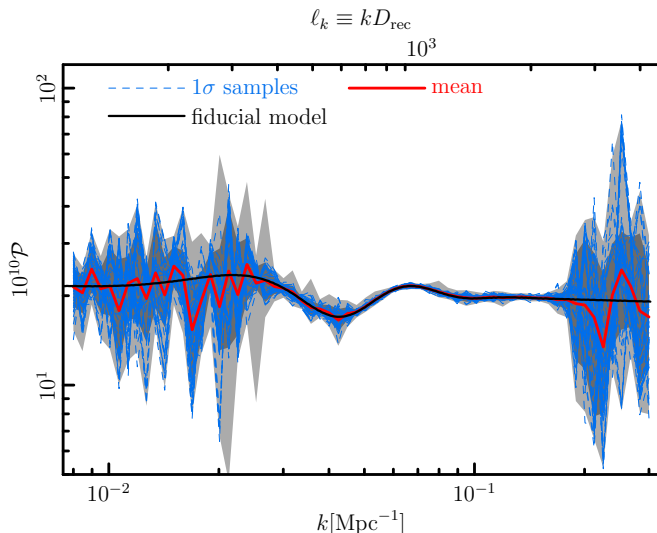


Figure 2. Reconstructed primordial power spectrum for the mock CMB data generated from the inflationary model in Eq. (3). The dashed sky-blue lines are randomly picked trajectories from the likelihood-ordered top 68.3% MCMC samples. The dark-gray and light-gray contours are marginalized 68.3% and 95.4% confidence level bounds, respectively.

C_ℓ^{XY} ($X, Y \in \{T, E\}$) are the model-dependent theoretical angular power spectra. They are given by $C_\ell^{XY} = C_\ell^{XY} + N_\ell^{XY}$, where C_ℓ^{XY} are the noise-free CMB power spectra calculated with the publicly available code CAMB (Lewis et al. 2000) and N_ℓ^{XY} are the noise spectra. To simulate the noise spectra, we assume a Gaussian beam shape and a sensitivity $50 \mu\text{K s}^{1/2}$ for temperature and $100 \mu\text{K s}^{1/2}$ for polarization, both integrated for five years. The hatted symbols \hat{C}_ℓ^{XY} represent the mock data predicted by the fiducial cosmology. To check whether the reconstruction method produces any bias, we do not add a realization of cosmic variance onto the mock data. Thus, any significant deviation from the fiducial model should be interpreted as a bias rather than a look-elsewhere effect. For the real data that we will discuss in the next section, the look-elsewhere effect cannot be avoided and weak “anomalies” should not be overly interpreted.

We apply the wavelet reconstruction method to the mock CMB data. An unbiased detection of the input power spectrum including the slow-roll violation signal is shown in Fig. 2. As shown Table 1, the other input cosmological parameters are also well recovered with no noticeable bias.

We leave more detailed interpretation of the reconstructed primordial power spectrum to the next section, where the real CMB data are investigated.

4. PLANCK + SH0ES + H0LICOW

Table 1. Marginalized constraints on cosmological parameters for mock data.

Parameter	fiducial	constraint
$\Omega_b h^2$	0.02238	$0.02233^{+0.00036}_{-0.00031}$
$\Omega_c h^2$	0.1201	$0.1202^{+0.0026}_{-0.0025}$
H_0 (km/s/Mpc)	67.3	$67.2^{+1.0}_{-1.0}$
τ_{re}	0.0543	$0.0542^{+0.0027}_{-0.0026}$

Table 2. Marginalized constraints on cosmological parameters for *Planck*+SH0ES+H0LiCow.

$\Omega_b h^2$	$0.0232^{+0.0005}_{-0.0005}$
$\Omega_c h^2$	$0.1169^{+0.0015}_{-0.0016}$
$100\theta_{MC}$	$1.04146^{+0.00037}_{-0.00037}$
τ_{re}	$0.063^{+0.010}_{-0.008}$
$\ln(10^{10} A_s)$	$3.060^{+0.019}_{-0.018}$
n_s	$0.995^{+0.010}_{-0.010}$
H_0 (km/s/Mpc)	$69.4^{+0.7}_{-0.7}$
$A_{3,-7}$	$-0.033^{+0.015}_{-0.015}$
other $A_{n,m}$ ’s	no detection beyond 2σ

To explicitly extract Hubble-tension-driven wavelet signals, we use jointly the SH0ES + H0LiCow constraint $H_0 = 73.82 \pm 1.10 \text{ km s}^{-1} \text{ Mpc}^{-1}$ (Wong et al. 2019) and the *Planck* final release of TT,TE,EE + lensing likelihood (Aghanim et al. 2019). Unlike the idealized mock CMB data that we discussed in the last section, the *Planck* likelihood contains many nuisance parameters to describe uncertainties in the foreground template, etc., all of which are marginalized over in our analysis.

Table 2 lists the marginalized 1σ constraints of cosmological parameters. The sixty-four wavelet expansion coefficients are mostly consistent with zero within 2σ , with only one 2.2σ exception $A_{3,-7} = -0.033 \pm 0.015$. The 2.2σ weak anomaly can be well explained by look-elsewhere effect for the many degrees of freedom we have injected into the model. Another weak anomaly is in the posterior of the reference $n_s = 0.995 \pm 0.010$, which is $\sim 2.7\sigma$ higher than the “no wavelet, no H_0 prior” case $n_s = 0.965 \pm 0.005$ (Aghanim et al. 2018). This can be explained by the known positive correlation between n_s and H_0 . More interestingly, it has been shown that the combination *Planck* + SH0ES favors a model with a scale invariant primordial power spectrum and $\sim 0.7 \pm 0.13$ extra relativistic species (Benetti et al. 2017; Benetti et al. 2018).

Finally, we would like to point out that these weak anomalies are not associated with the wavelet reconstruction method or our particular choice of the wavelet

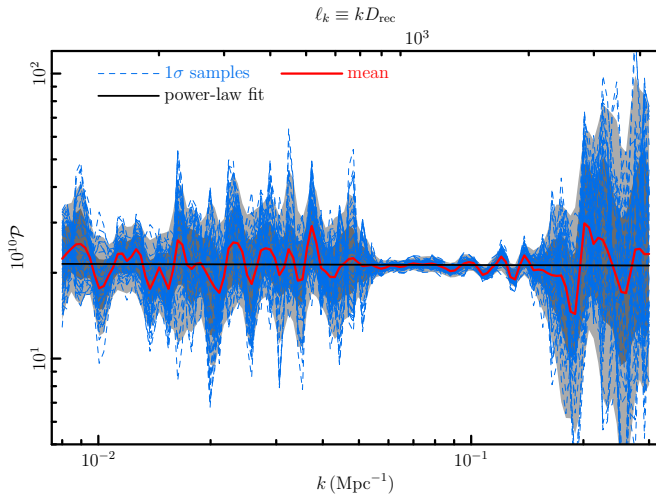


Figure 3. Reconstructed primordial power spectrum for *Planck*+SH0ES+H0LiCow. The dashed sky-blue lines are randomly picked trajectories from the likelihood-ordered top 68.3% MCMC samples. The dark-gray and light-gray contours are marginalized 68.3% and 95.4% confidence level bounds, respectively.

mother function, as the anomalies do not show up in the test with mock CMB data where the look-elsewhere effect is avoided on purpose.

In Fig. 3 we again visualize the reconstructed $\mathcal{P}(k)$ trajectories. The non-deviation from a power-law spectrum is consistent with the posteriors of the A_{mn} parameters. The constraints are worse than the test case with mock CMB data, because the real *Planck* data has foreground modeling uncertainties (especially for the polarization) and a slightly higher noise level than what we assumed in Sec. 3.

Compared to the 12-knot cubic spline reconstruction in section 6.3 of Akrami et al. (2018b), our wavelet analysis, by construction, picks out more local and sharper features. The high-frequency wiggling in $\mathcal{P}(k)$ is driven, or at least partially driven by the statistical fluctuations in CMB power spectra. In Fig 4 we show how the wavelet trajectories follow statistical fluctuations in the temperature angular power spectrum D_ℓ^{TT} , allowed by cosmic variance at low and intermediate ell's. At higher ell's, the trajectories converge due to a much smaller cosmic variance. These features can also be seen in the left and middle parts of Fig 3. The large scattering in the right part of Fig 3 corresponds to the unconstrained power on small scales (high- k) beyond *Planck* resolution.

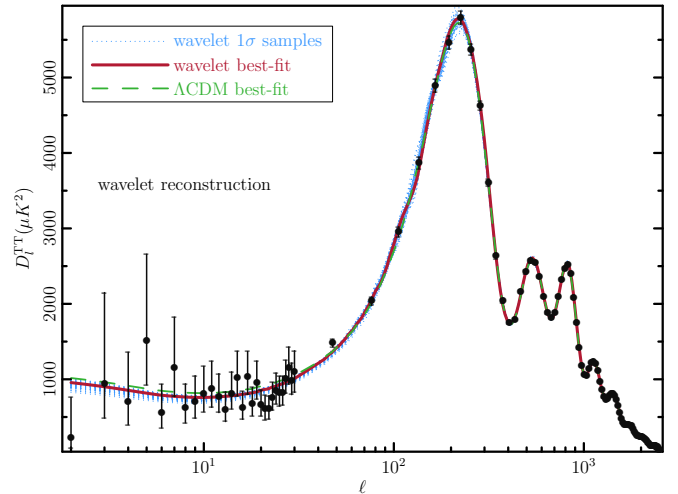


Figure 4. CMB temperature power $D_\ell^{\text{TT}} \equiv \frac{\ell(\ell+1)}{2\pi} C_\ell^{\text{TT}}$, where C_ℓ^{TT} is the angular power spectrum of temperature fluctuations. The dotted sky-blue lines are randomly picked trajectories from the likelihood-ordered top 68.3% MCMC samples. The solid red line is the best-fit for wavelet expansion of $\mathcal{P}(k)$, whereas the dashed green line is the best-fit for the minimal six-parameter Λ CDM with power-law $\mathcal{P}(k)$.

For the Hubble constant, we obtain a *Planck* + SH0ES + H0LiCow joint constraint: $H_0 = 69.4 \pm 0.7 \text{ km s}^{-1} \text{ Mpc}^{-1}$. Because the posterior is very close to Gaussian, we can approximately remove the SH0ES + H0LiCow contribution and obtain a *Planck*-only constraint, as shown in Fig. 5. For a comparison, we also plot the *Planck* constraint for the standard Λ CDM power-law case as well as the 12-knot-spline case, which we obtain by repeating the calculations in Akrami et al. (2018b). We find that allowing more features in the primordial power spectrum, either local and band-limited as in the wavelet case, or just low-pass filtered as in the 12-knot-spline case, in general pushes the mean H_0 towards an even smaller value, which balances out the increased uncertainty and keeps the Hubble tension at roughly the same level. More specifically, the tension between *Planck* and SH0ES + H0LiCow is 4.9σ for the wavelet analysis, and 5.3σ for the 12-knot-spline.

5. CONCLUSION AND DISCUSSION

To check the robustness of the wavelet analysis method, we repeated our calculation with 2nd order Daubechies basis, and found no significant variations in the results. We thus conclude that the Hubble tension cannot be eased by band-limited features in the primordial power spectrum with $\Delta \ln k \gtrsim 0.1$.

Ideally, the wavelet analysis, if expanded to infinite order, is equivalent to many other binning, expan-

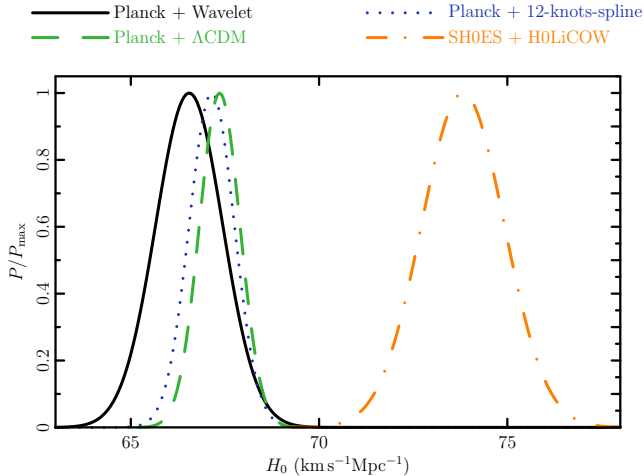


Figure 5. Comparison of H_0 constraints.

sion and interpolation methods. Practically, however, one has to introduce a cut in expansion order or a

smoothing scheme to reduce the dimension of parameter space and to achieve MCMC convergence. The cut or smoothing schemes in different methods introduce model-dependent priors. In our wavelet analysis, the cut of expansion order leads to a prior that captures the local and band-limited features that naturally arise from various inflationary processes beyond slow-roll. Indeed, if not limited by the physical prior, a deconvolution scheme can map the H_0 -discordance in the CMB power spectrum to the primordial power spectrum and ease the Hubble tension (Hazra et al. 2019).

6. ACKNOWLEDGMENTS

We thank J. Richard Bond, Lev Kofman and Pascal Vaudrevange for many useful discussions in the memorable days in Toronto. This work is supported by Sun Yat-sen University Research Starting Grant 71000-18841232.

APPENDIX

A. THE CALCULATION OF DAUBECHIES MOTHER WAVELET

The mother wavelet $\Psi_{0,0}(t)$ is constructed from the scaling function $\phi(t)$ (or father wavelet) via

$$\Psi_{0,0}(t) = \sqrt{2} \sum_{k=0}^{2n-1} (-1)^k c_{2n-1-k} \phi(2t - k), \quad t \in (-\infty, \infty), \quad (\text{A1})$$

where n is the order of the wavelet system. The scaling function ϕ is defined recursively through the use of dilation equations. The basic dilation equation reads

$$\phi_m(t) = \sqrt{2} \sum_{k=0}^{2n-1} c_k \phi_{m-1}(2t - k). \quad (\text{A2})$$

It is a two-scale or dyadic difference equation. The starting point of recursion $\phi_{-1}(t)$ is defined as the Haar father wavelet, which is equal to 1 in the interval $[0, 1]$ and vanishes elsewhere. When the recursion order $m \rightarrow \infty$, $\phi_m(t)$ converges to the scaling function $\phi(t)$.

The numerical values of the filter coefficients c_k can be calculated via the algorithm named after Daubechies (Daubechies 1998). Defining the polynomial

$$P_n(y) = \sum_{k=0}^{n-1} \binom{n-1+k}{k} y^k, \quad (\text{A3})$$

one can calculate numerically the (complex) roots of

$$P_n\left(\frac{1}{2} - \frac{1}{4z} - \frac{z}{4}\right), \quad (\text{A4})$$

where z is an arbitrary complex variable. Selecting those roots r_i inside the unit circle ($\|r_i\| < 1$), one obtains the filter coefficients by identifying the coefficients \tilde{c}_k of

$$(z+1)^n \prod_{i=1}^{n-1} (z - r_i) \equiv \sum_{k=0}^{2n-1} \tilde{c}_k z^{2n-k-1}. \quad (\text{A5})$$

After normalization, the coefficients are

$$c_k = \frac{\tilde{C}_k}{\sqrt{\sum_{k=0}^{2n-1} \tilde{C}_k^2}}. \quad (\text{A6})$$

For example, the $c_0 \sim c_7$ of the 4th order Daubechies wavelet system are: 0.230378, 0.714847, 0.630881, -0.0279838 , -0.1870348 , 0.0308414, 0.0328830, -0.0105974 .

REFERENCES

- Abbott, T. M. C., et al. 2019, *Mon. Not. Roy. Astron. Soc.*, 483, 4866, doi: [10.1093/mnras/sty3351](https://doi.org/10.1093/mnras/sty3351)
- Adhikari, S., & Huterer, D. 2020, *Physics of the Dark Universe*, 28, 100539, doi: [10.1016/j.dark.2020.100539](https://doi.org/10.1016/j.dark.2020.100539)
- Aghanim, N., et al. 2018. <https://arxiv.org/abs/1807.06209>
- . 2019. <https://arxiv.org/abs/1907.12875>
- Akrami, Y., et al. 2018a. <https://arxiv.org/abs/1807.06205>
- . 2018b. <https://arxiv.org/abs/1807.06211>
- . 2019. <https://arxiv.org/abs/1905.05697>
- Alexander, S., & McDonough, E. 2019, *Physics Letters B*, 797, 134830, doi: [10.1016/j.physletb.2019.134830](https://doi.org/10.1016/j.physletb.2019.134830)
- Benetti, M., Graef, L. L., & Alcaniz, J. 2018, *Journal of Cosmology and Astroparticle Physics*, 2018, 066066, doi: [10.1088/1475-7516/2018/07/066](https://doi.org/10.1088/1475-7516/2018/07/066)
- Benetti, M., Graef, L. L., & Alcaniz, J. S. 2017, *JCAP*, 2017, 003, doi: [10.1088/1475-7516/2017/04/003](https://doi.org/10.1088/1475-7516/2017/04/003)
- Bhattacharyya, A., Alam, U., Pandey, K. L., Das, S., & Pal, S. 2019, *The Astrophysical Journal*, 876, 143, doi: [10.3847/1538-4357/ab12d6](https://doi.org/10.3847/1538-4357/ab12d6)
- Blinov, N., Keith, C., & Hooper, D. 2020, arXiv e-prints, arXiv:2004.06114. <https://arxiv.org/abs/2004.06114>
- Bolejko, K. 2018, *Physical Review D*, 97, doi: [10.1103/physrevd.97.103529](https://doi.org/10.1103/physrevd.97.103529)
- Carneiro, S., de Holanda, P., Pigozzo, C., & Sobreira, F. 2019, *Physical Review D*, 100, doi: [10.1103/physrevd.100.023505](https://doi.org/10.1103/physrevd.100.023505)
- Chiang, C.-T., & Slosar, A. 2018, arXiv e-prints, arXiv:1811.03624. <https://arxiv.org/abs/1811.03624>
- Daubechies, I. 1998, *Computers in Physics*, 6, 1671
- D’Eramo, F., Ferreira, R. Z., Notari, A., & Bernal, J. L. 2018, *Journal of Cosmology and Astroparticle Physics*, 2018, 014014, doi: [10.1088/1475-7516/2018/11/014](https://doi.org/10.1088/1475-7516/2018/11/014)
- Di Valentino, E., Melchiorri, A., & Mena, O. 2017, *Physical Review D*, 96, doi: [10.1103/physrevd.96.043503](https://doi.org/10.1103/physrevd.96.043503)
- Di Valentino, E., Melchiorri, A., Mena, O., & Vagnozzi, S. 2019. <https://arxiv.org/abs/1908.04281>
- Di Valentino, E., et al. 2018, *Physical Review D*, 97, doi: [10.1103/physrevd.97.043513](https://doi.org/10.1103/physrevd.97.043513)
- Domnech, G., & Kamionkowski, M. 2019, *Journal of Cosmology and Astroparticle Physics*, 2019, 040040, doi: [10.1088/1475-7516/2019/11/040](https://doi.org/10.1088/1475-7516/2019/11/040)
- Gil-Marín, H., Percival, W. J., Cuesta, A. J., et al. 2016, *MNRAS*, 460, 4210, doi: [10.1093/mnras/stw1264](https://doi.org/10.1093/mnras/stw1264)
- Graef, L. L., Benetti, M., & Alcaniz, J. S. 2019, *Physical Review D*, 99, doi: [10.1103/physrevd.99.043519](https://doi.org/10.1103/physrevd.99.043519)
- Guo, R.-Y., Zhang, J.-F., & Zhang, X. 2019, *Journal of Cosmology and Astroparticle Physics*, 2019, 054054, doi: [10.1088/1475-7516/2019/02/054](https://doi.org/10.1088/1475-7516/2019/02/054)
- Handley, W. J., Lasenby, A. N., Peiris, H. V., & Hobson, M. P. 2019, *Phys. Rev. D*, 100, 103511, doi: [10.1103/PhysRevD.100.103511](https://doi.org/10.1103/PhysRevD.100.103511)
- Hazra, D. K., Shafieloo, A., & Smoot, G. F. 2013, *JCAP*, 1312, 035, doi: [10.1088/1475-7516/2013/12/035](https://doi.org/10.1088/1475-7516/2013/12/035)
- Hazra, D. K., Shafieloo, A., & Souradeep, T. 2019, *JCAP*, 1904, 036, doi: [10.1088/1475-7516/2019/04/036](https://doi.org/10.1088/1475-7516/2019/04/036)
- Jedamzik, K., & Pogosian, L. 2020, arXiv e-prints, arXiv:2004.09487. <https://arxiv.org/abs/2004.09487>
- Karwal, T., & Kamionkowski, M. 2016, *Physical Review D*, 94, doi: [10.1103/physrevd.94.103523](https://doi.org/10.1103/physrevd.94.103523)
- Kovács, A., Beck, R., Szapudi, I., et al. 2020, arXiv e-prints, arXiv:2004.02937. <https://arxiv.org/abs/2004.02937>
- Lewis, A., & Bridle, S. 2002, *Physical Review D*, 66, 103511
- Lewis, A., Challinor, A., & Lasenby, A. 2000, *Astrophys. J.*, 538, 473, doi: [10.1086/309179](https://doi.org/10.1086/309179)
- Li, X., & Shafieloo, A. 2019, *Astrophys. J.*, 883, L3, doi: [10.3847/2041-8213/ab3e09](https://doi.org/10.3847/2041-8213/ab3e09)
- Lin, M.-X., Benevento, G., Hu, W., & Raveri, M. 2019a, *Phys. Rev.*, D100, 063542, doi: [10.1103/PhysRevD.100.063542](https://doi.org/10.1103/PhysRevD.100.063542)
- Lin, M.-X., Raveri, M., & Hu, W. 2019b, *Phys. Rev.*, D99, 043514, doi: [10.1103/PhysRevD.99.043514](https://doi.org/10.1103/PhysRevD.99.043514)
- Liu, M., Huang, Z., Luo, X., et al. 2019, arXiv e-prints, arXiv:1912.00190. <https://arxiv.org/abs/1912.00190>
- Macauley, E., et al. 2019, *MNRAS*, 486, 2184, doi: [10.1093/mnras/stz978](https://doi.org/10.1093/mnras/stz978)
- Meerburg, P. D., Wijers, R. A. M. J., & van der Schaar, J. P. 2012, *Monthly Notices of the Royal Astronomical Society*, nono, doi: [10.1111/j.1365-2966.2011.20311.x](https://doi.org/10.1111/j.1365-2966.2011.20311.x)
- Miao, H., & Huang, Z. 2018, *The Astrophysical Journal*, 868, 20, doi: [10.3847/1538-4357/aae523](https://doi.org/10.3847/1538-4357/aae523)
- Mukhanov, V. F. 1988, *Zhurnal Eksperimentalnoi i Teoreticheskoi Fiziki*, 94, 1

- Mukherjee, P., Hobson, M. P., & Lasenby, A. 2000, *Monthly Notices of the Royal Astronomical Society*, 318, 1157
- Mukherjee, P., & Wang, Y. 2003a, *Astrophys. J.*, 593, 38, doi: [10.1086/376500](https://doi.org/10.1086/376500)
- . 2003b, *The Astrophysical Journal*, 598, 779
- Pan, S., Yang, W., Di Valentino, E., Shafieloo, A., & Chakraborty, S. 2019. <https://arxiv.org/abs/1907.12551>
- Pando, J., Valls-gabaud, D., & Fang, L. 1998, *Physical Review Letters*, 81, 4568
- Panpanich, S., Burikham, P., Ponglertsakul, S., & Tannukij, L. 2019. <https://arxiv.org/abs/1908.03324>
- Perlmutter, S., et al. 1999, *ApJ*, 517, 565, doi: [10.1086/307221](https://doi.org/10.1086/307221)
- Poulin, V., Smith, T. L., Karwal, T., & Kamionkowski, M. 2019, *Physical Review Letters*, 122, doi: [10.1103/physrevlett.122.221301](https://doi.org/10.1103/physrevlett.122.221301)
- RÁCZ, G., DOBOS, L., BECK, R., SZAPUDI, I., & CSABAI, I. 2017, *MNRAS*, 469, L1, doi: [10.1093/mnrasl/slx026](https://doi.org/10.1093/mnrasl/slx026)
- Riess, A. G., Casertano, S., Yuan, W., Macri, L. M., & Scolnic, D. 2019, *The Astrophysical Journal*, 876, 85
- Riess, A. G., et al. 1998, *AJ*, 116, 1009, doi: [10.1086/300499](https://doi.org/10.1086/300499)
- Riess, A. G., et al. 2016, *ApJ*, 826, 56, doi: [10.3847/0004-637X/826/1/56](https://doi.org/10.3847/0004-637X/826/1/56)
- . 2018a, *ApJ*, 855, 136, doi: [10.3847/1538-4357/aaadb7](https://doi.org/10.3847/1538-4357/aaadb7)
- . 2018b, *ApJ*, 861, 126, doi: [10.3847/1538-4357/aac82e](https://doi.org/10.3847/1538-4357/aac82e)
- Rossi, M., Ballardini, M., Braglia, M., et al. 2019. <https://arxiv.org/abs/1906.10218>
- Sasaki, M. 1986, *Progress of Theoretical Physics*, 76, 1036, doi: [10.1143/PTP.76.1036](https://doi.org/10.1143/PTP.76.1036)
- Scolnic, D. M., et al. 2018, *Astrophys. J.*, 859, 101, doi: [10.3847/1538-4357/aab9bb](https://doi.org/10.3847/1538-4357/aab9bb)
- Shafieloo, A., Souradeep, T., Manimaran, P., Panigrahi, P. K., & Rangarajan, R. 2007, *Phys. Rev.*, D75, 123502, doi: [10.1103/PhysRevD.75.123502](https://doi.org/10.1103/PhysRevD.75.123502)
- Shajib, A. J., et al. 2019. <https://arxiv.org/abs/1910.06306>
- Sola, J., Gomez-Valent, A., Perez, J. d. C., & Moreno-Pulido, C. 2019. <https://arxiv.org/abs/1909.02554>
- Starobinsky, A. A. 1983, *Pisma v Astronomicheskii Zhurnal*, 9, 579
- Tocchinivalentini, D., Hoffman, Y., & Silk, J. 2006, *Monthly Notices of the Royal Astronomical Society*, 367, 1095
- Troxel, M. A., et al. 2018, *Phys. Rev.*, D98, 043528, doi: [10.1103/PhysRevD.98.043528](https://doi.org/10.1103/PhysRevD.98.043528)
- Vattis, K., Koushiappas, S. M., & Loeb, A. 2019, *PhRvD*, 99, 121302, doi: [10.1103/PhysRevD.99.121302](https://doi.org/10.1103/PhysRevD.99.121302)
- Verde, L., & Peiris, H. 2008, *Journal of Cosmology & Astroparticle Physics*, 7, 807
- Verde, L., Peiris, H. V., & Jimenez, R. 2006, *Journal of Cosmology and Astro-Particle Physics*, 1, 19, doi: [10.1088/1475-7516/2006/01/019](https://doi.org/10.1088/1475-7516/2006/01/019)
- Wong, K. C., et al. 2019. <https://arxiv.org/abs/1907.04869>
- Yang, W., Mukherjee, A., Di Valentino, E., & Pan, S. 2018a, *Physical Review D*, 98, doi: [10.1103/physrevd.98.123527](https://doi.org/10.1103/physrevd.98.123527)
- Yang, W., Pan, S., Di Valentino, E., et al. 2018b, *JCAP*, 1809, 019, doi: [10.1088/1475-7516/2018/09/019](https://doi.org/10.1088/1475-7516/2018/09/019)
- Ye, G., & Piao, Y.-S. 2020, *PhRvD*, 101, 083507, doi: [10.1103/PhysRevD.101.083507](https://doi.org/10.1103/PhysRevD.101.083507)
- Zeng, C., et al. 2019, *Physical Review D*, 99, doi: [10.1103/physrevd.99.043517](https://doi.org/10.1103/physrevd.99.043517)